

# Funicular Flexible Crawler for Colonoscopy\*

Jun-ya Nagase, *Member, IEEE*, Fumika Fukunaga, Keiji Ogawa, and Norihiko Saga, *Member, IEEE*

**Abstract**— The number of people with cancer of the large intestine has been increasing steadily. According to The Global Cancer Observatory, its prevalence is second among all cancer types in world statistics over the past five years. Early detection and treatment of diseases by colonoscopy can enable complete recovery. Nevertheless, conventional colonoscopes require extremely high skill of the doctors who use them. Moreover, their invasiveness in the colon is high. Therefore, many robots to facilitate colonoscopy-related operations have been developed recently. Unfortunately, no practical system exists which can truly overcome the proven effectiveness and lower costs presented by conventional colonoscopes. We therefore propose a novel autonomous propulsion mechanism for colonoscopy named the “Funicular Flexible Crawler.” It is suitable for propulsion through narrow spaces because it is driven by multiple small diameter crawler units connected to a flexible shaft. Experimentation with a large intestine phantom confirmed that the flexible crawler can run from the rectum to the cecum. As described herein, this propulsion mechanism is applicable for self-traveling colonoscopy.

**Index Terms**—Colonoscopy, crawler belt, flexible shaft, large intestine

## I. INTRODUCTION

IN Japan, colorectal cancer is the third most common cause of cancer death in men and the first most common cause in women [1]. Early detection of such diseases supports complete recovery. The five-year survival rate is 95% if cancer can be found while it remains in the large intestine. To conduct examinations for colon cancer detection, a doctor inserts a colonoscope through the anus. The large intestine is non-fixed, with high flexibility and complicated shape. Therefore, doctors must have extremely developed skills to insert a conventional colonoscope, which consists of a distal bending tip, a colonoscope body, tendon knobs, connector, biopsy forceps, and high-resolution mini-camera at the end of the distal bending tip. A doctor must use both hands to insert such colonoscopes into the large intestine: the strong hand advances the endoscope while the supporting hand bends the tip to direct it. Typically, patients feel pain and discomfort during procedures. Conventional colonoscopy has mainly two colonoscope insertion methods as depicted in Fig. 1: a loop method and a non-loop method [2], [3]. These methods are commonly used at

clinical sites. The loop method is likely to be painful because of hyperextension of the intestines. The non-loop method suppresses hyperextension and causes less pain, but it is very difficult to master. Therefore, doctors must have extremely high skills for colonoscopy insertion. The insertion time and load on the large intestine strongly depend on their skill.

Given such circumstances, capsule endoscopes have been developed as painless inspection devices [4]–[7]. Capsule-type endoscopes can be swallowed, after which they move from the mouth to the anus by peristaltic waves. Consequently, diagnosis of small intestine disorders is now possible. Examinations are painless and safe, but no active diagnosis or MIS is possible because a locomotive mechanism is lacking [8]. For that reason, their application is limited.

Several developed inchworm-like endoscopic robots are driven by shape memory alloy (SMA) actuator, DC motor, or a pneumatic actuator [9]–[11]. Theoretically, through rhythmic control of their actuators, these robots can move forward and backward similarly to an inchworm. Nevertheless, such robots move very slowly through the intestinal tract because the colon is slippery and loosely constrained [9], [10]. Endotics system showed superiority in pain reduction versus conventional colonoscopy, but a relatively low cecal intubation rate need to be overcome [11].

Conventional wired endoscopes are still necessary for medical procedures for precise diagnosis, polyp removal, and so on. They are more reliable and are usually used to diagnose the colon. Therefore, several active wired endoscopes have been studied. One report by Alcaide et al. [12] describes locomotion of their robot, which mimics an earthworm’s peristaltic motion and which uses SMA actuators. Nakamura et al. [13] also developed a peristaltic crawling robot using fiber-reinforced artificial muscles for colonoscopy. However, they have difficulty moving quickly in phantoms of large intestines. Wakimoto and Suzumori [14] developed a propulsion device using travelling waves driven by a pneumatic actuator and attempted to apply it to an endoscope. However, it cannot move independently.

For this study, we aimed at implementation of a semi-autonomous colonoscopic device with high running performance and safety in a large intestine. We developed a cylindrical crawler robot [15],[16] as presented in Fig. 2. The tracked crawler mechanism propels the robot by driving multiple crawler belts in axial symmetry to a cylindrical frame with a single actuator via a single worm. Consequently, it has a much simpler structure than that of a conventional tracked crawler mechanism with complicated structures and many actuators [17]–[19]. Our earlier device [20] can propel itself in narrow pipes of 50 mm inner diameter. Herein, we propose a

\*Research supported by Grant-in-Aid for Scientific Research (C)(No. 17K01429).

\*Jun-ya Nagase and Keiji Ogawa are with Mechanical and Systems Engineering, Science and Technology, Ryukoku University, Shiga, Japan. Fumika Fukunaga was with Mechanical and Systems Engineering, Science and Technology, Ryukoku University, Shiga, Japan. She is now with Johnson and Johnson, Tokyo, Japan. Norihiko Saga is with Human System Interaction, Kwansai Gakuin University, Hyogo, Japan. (correspondence e-mail: [nagase@rins.ryukoku.ac.jp](mailto:nagase@rins.ryukoku.ac.jp)).

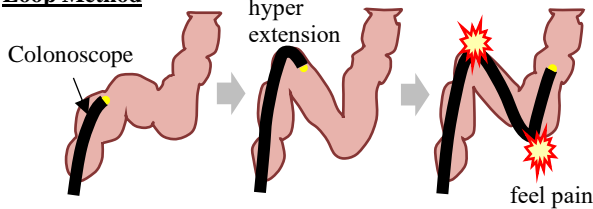
funicular flexible crawler mechanism with 16.4 mm outer diameter based on our earlier crawler used for colonoscopy.

Section II describes the structure and driving mechanism of the funicular flexible crawler. Section III explains the basic characteristics of the crawler unit for propulsion. Section IV describes the steering characteristics of crawler unit for turning. Section V explains the running characteristics of the funicular flexible crawler.

## II. FUNICULAR FLEXIBLE CRAWLER STRUCTURE AND DRIVING MECHANISM

Fig. 3 presents the structure of the funicular flexible crawler: The flexible crawler includes an actuation unit, crawler units for propulsion, a crawler unit for turning, a flexible inner shaft, and a flexible outer shaft. The actuation unit has a geared motor. The geared motor output shaft is connected to a flexible inner shaft through a coupling. Multiple crawler units used for propulsion are arranged in the flexible inner shaft.

### Loop Method



### Non Loop Method

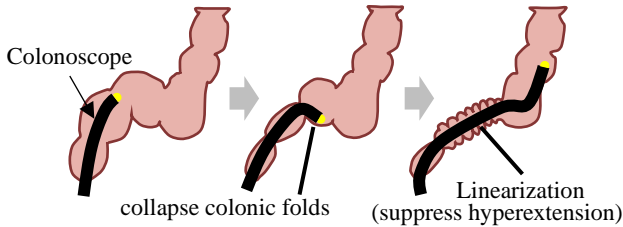


Fig. 1. Conventional colonoscopy

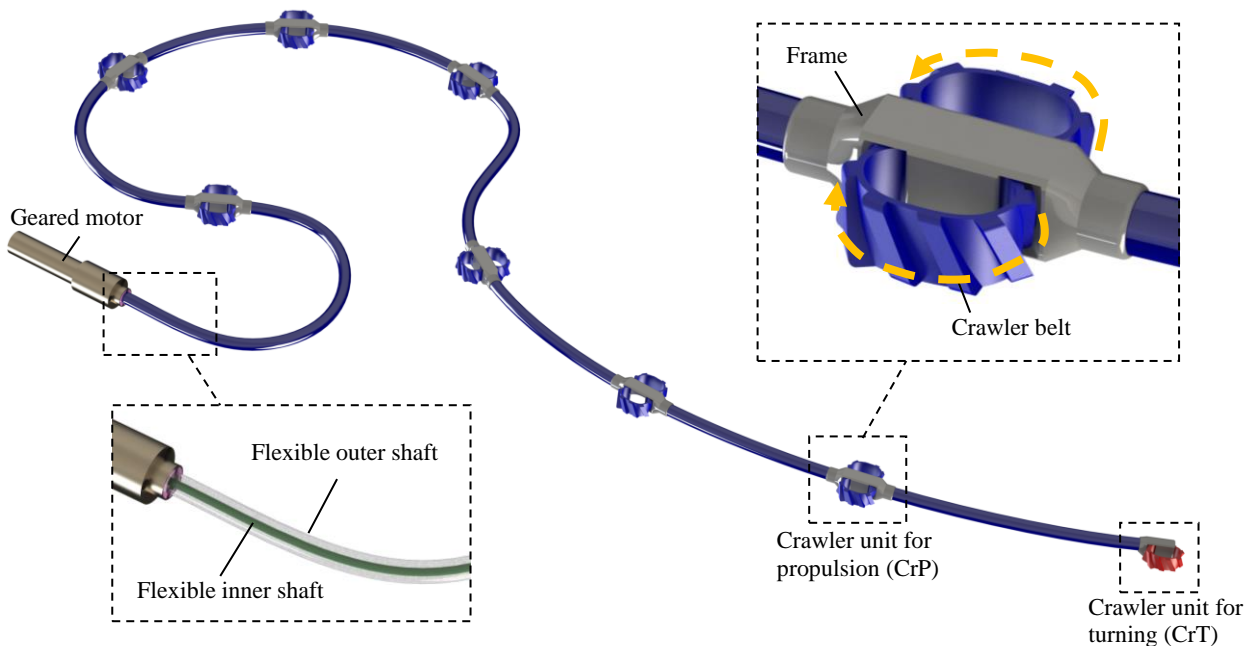


Fig. 3. Funicular flexible crawler proposed in this study.

Fig. 4 portrays a section of the crawler unit used for propulsion. The unit comprises a worm, crawler belts, and a frame. Bearings at both ends support the worm, arranged inside the frame. Both worm ends are connected to a flexible inner shaft. Two crawler belts are spaced asymmetrically around the longitudinal axis of the cylindrical frame. Each crawler belt is wound around the frame: both ends are connected, producing a loop. Additionally, teeth having a rake angle corresponding to the lead angle of the worm tooth are formed on the crawler belt outer surface. A crawler unit for turning is connected to the distal end of the flexible inner shaft. The crawler has a single crawler belt. The frame installed in the crawler unit supports one end of the worm. Other structural features of the crawler unit for turning are the same as those of the crawler unit for propulsion. A hollow flexible outer shaft is arranged between each crawler unit and between the motor frame and the crawler unit. It is positioned around the flexible inner shaft.

Next, we describe the flexible crawler driving mechanism. First, by driving the gearmotor installed in the actuator unit, torque is generated on the flexible inner shaft. Then the worms connected to the flexible inner shaft rotate so that the crawler belt engaged with the worm rotates longitudinally. Finally, propulsive force is generated in the flexible crawler by

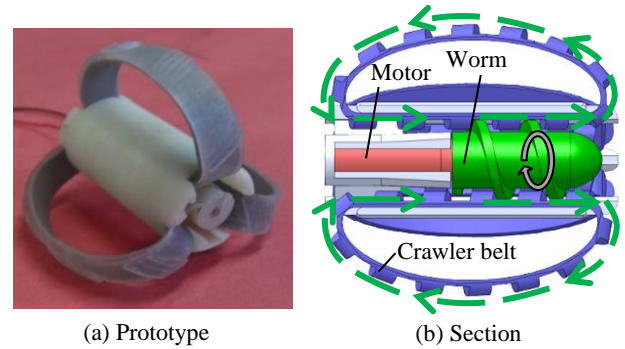


Fig. 2. Amoeba-inspired cylindrical crawler mechanism locomotion proposed earlier.

frictional force acting on the ground contact surface from the crawler belts.

Multiple crawlers can be arranged on the shaft. Therefore, a propulsive force can be generated throughout the colonoscope. The crawler belts are soft rubber belts that are curved to the outside of the frame. Therefore, the crawler can move easily along the irregular intestinal inside wall. Furthermore, a single gear motor is located at one end of the flexible shaft on the outside of the crawler. Therefore, during colonoscopy, one can arrange the gear motor outside the body so that the crawler unit can be greatly miniaturized. For the flexible crawler prototype described in Section V, 16.4 mm outer diameter was achieved: it is the narrowest crawler structure ever reported.

For conventional wired colonoscopes, pushing force of the hand must be transmitted directly to the end of the scope during insertion. Therefore, the colonoscope has high bending rigidity, putting a large burden on the large intestine. By contrast, this flexible crawler can run along the contours of the large intestine while generating a propulsive force on the endoscope by a crawler unit arranged on several flexible shafts. It can therefore alleviate the load on the large intestine.

### III. CRAWLER UNIT FOR PROPULSION

#### A. Relation between crawler belt length and traction force

The traction force generated in each crawler unit section propels the flexible crawler. The crawler traction force is believed to be attributable to the crawler belt properties. For this reason, this study must investigate the relation between the crawler belt properties and the traction force. However, the large intestine structure is extremely complex. It has many folds in its inner wall. Moreover, the inner diameter and the shape differ depending on the location in the apparatus. Therefore, quantitative evaluation of the traction force characteristics in the large intestine is difficult. First, we examined the relation between belt length and traction force using an acrylic pipe to assess the fundamental characteristics of the traction force.

A schematic diagram of the experimental device for traction force measurement and the crawler unit used in the experiment is portrayed in Fig. 5. For this experiment, the traction force of the crawler unit driving in an acrylic pipe was measured using a force gauge (FGP-5; Nidec Corp.) fixed to the ground, as portrayed in Fig. 5. The 28 mm inner diameter acrylic pipe is connected vertically to the force gauge tip. A lubricant was used in the pipe to simulate a wet condition. The gear motor is fixed to the wall at the top of the pipe. The crawler unit is connected to the gear motor through a flexible shaft. The crawler unit's total length is 44 mm. The outermost diameter of the crawler is 16.4 mm. The 8-mm-wide silicone rubber crawler belt is in an epoxy resin frame.

The respective rubber hardnesses of durometer type A were 50, 60, 70, and 80. Generally speaking, Young's modulus increases when durometer type A increases. The respective numbers of belt teeth were 5, 6, 7, 8, 9, 10, 11, and 12. The pitch lengths of all belts were 7.3 mm. The belt length is proportional to the number of belt teeth because the crawler belt length is the pitch length multiplied by the number of belt teeth.

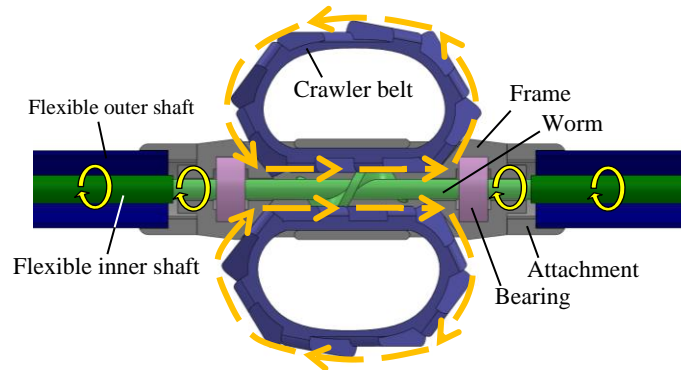


Fig. 4. Section of a crawler unit.

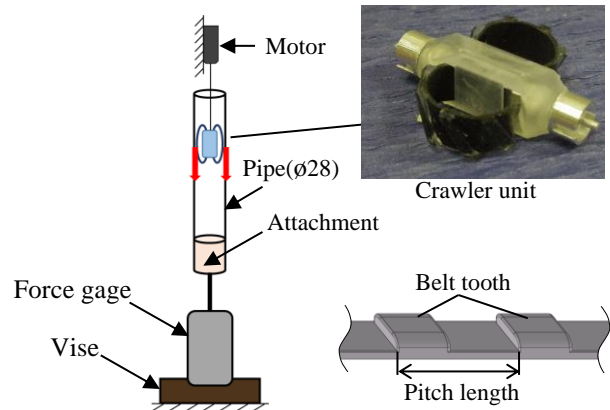


Fig. 5. System for measuring crawler traction force.

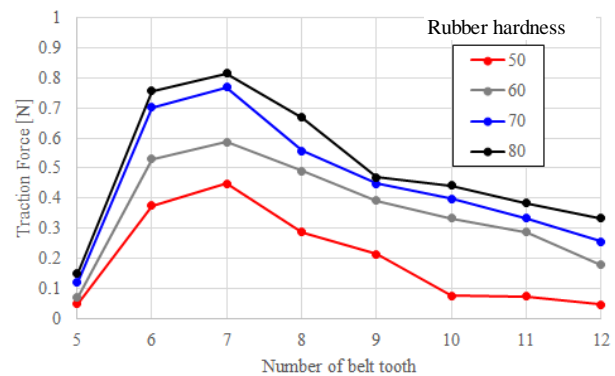


Fig. 6. Belt teeth number and traction force on each rubber hardness (Type A durometer).

The maximum traction force was measured five times for each belt. Then the average of five measurements was taken as the traction force measurement result. Fig. 6 presents the relation between the number of the belt teeth and traction force for respective rubber hardnesses (Type A durometer): The black, blue, gray and red lines respectively represent rubber hardnesses of 80, 70, 60, and 50. Slippage between the belt and the pipe occurred in this experiment. The traction force, which increases with belt hardness, has a local maximum value with respect to the belt length. The belt length exhibiting the strongest traction force was independent of the belt hardness.

#### B. Elastic force of the crawler belt

The frictional force between the elastically deformed crawler

belt and the ground contact surface generates the flexible crawler traction force. Therefore, the traction force of the crawler unit probably depends on the crawler belt elastic force. The elastic force characteristics of the crawler belt were measured to investigate the mechanism by which the belt elastic force influences the crawler unit traction force.

Fig. 7 presents the experimental system used to measure the crawler unit elastic force. In the experiment, with the crawler unit fixed at both ends with a vise, the radial elastic force was measured when the plate was pressed against the crawler belt. The pushing amount of the crawler belt was set as equal to the radial deformation amount of the belt when the crawler unit was inside a  $\phi 28$  mm pipe. The respective numbers of the belt teeth were 5, 6, 7, 8, 9, 10, 11, and 12. The rubber hardness of durometer type A was 80. The elastic force was measured five times for each belt. Then the average of five measurements was taken as the elastic force measurement result.

Fig. 8 presents the measurement results. As with the traction characteristics, the elastic force exhibited a characteristic of having a local maximum value with respect to the belt length. Furthermore, as with the traction characteristics, the belt with seven teeth showed the strongest elastic force. Apparently, the traction force characteristics of the crawler unit are dominated by elastic force characteristics.

Next, we present some theoretical discussion of the elastic force characteristics. The crawler belt is made of rubber. Therefore, its material nonlinearity is strong. The crawler belt deforms considerably. Therefore, its geometrical nonlinearity is also strong. The crawler belt characteristics considering such nonlinearity cannot be analyzed theoretically. In this study, using a simplified linear model of the crawler belt, as presented in Fig. 9, we discuss the crawler belt elastic force having a local maximum value with respect to the belt length.

The relation between belt length  $l$  and radial direction elastic force  $W$  can be expressed as the following equations referred from the literature [21].

$$W = \alpha E \frac{D_y}{\sqrt{3}} \quad (1)$$

$$\alpha = \frac{8\pi^3}{\left(\frac{\pi}{4} - \frac{2}{\pi}\right) l} \quad (2)$$

where  $E$  denotes Young's modulus,  $D_y$  represents belt deformation in the radial direction, and  $l$  signifies the moment of inertia of area. Belt deformation  $D_y$  in the radial direction is written geometrically as the following equation.

$$D_y = \frac{l}{\pi} + t + r_w - r_p \quad (3)$$

From Eqs. (1)–(3), the relation between the belt length  $l$  and the elastic force  $W$  for pipe radius  $r_p$  can be derived as follows.

$$W = \frac{\alpha E}{l^2} \left\{ \frac{1}{\pi} + \frac{1}{l} (t + r_w - r_p) \right\} \quad (4)$$

Regarding Eq. (4), when the belt length  $l$  satisfies Eq. (5), Eq. (6)

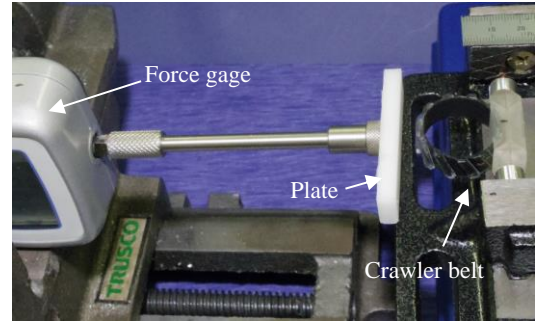


Fig. 7. System for measuring the crawler unit elastic force.

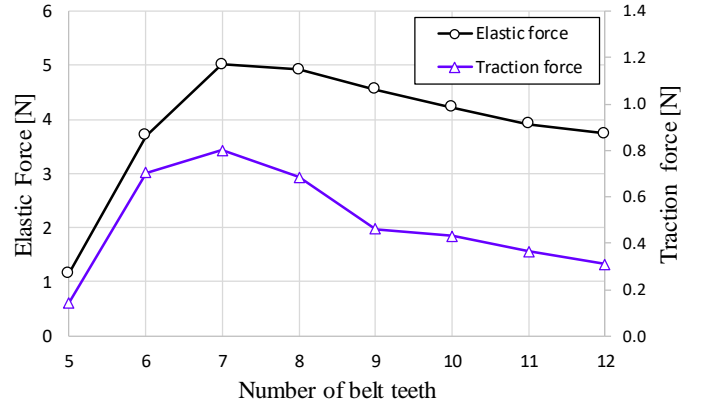


Fig. 8. Elastic and traction forces measured for different numbers of belt teeth.

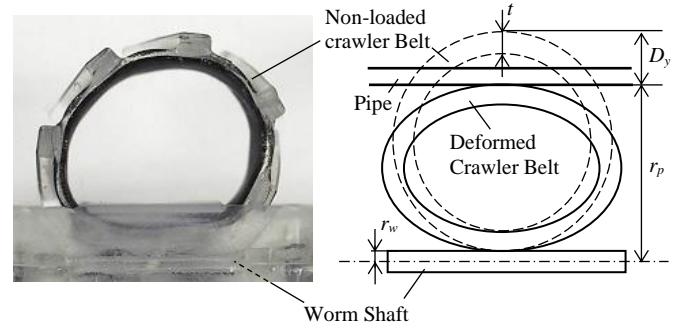


Fig. 9. Schematic diagram of the crawler belt and worm shaft for theoretical analysis.

is satisfied.

$$l = \frac{3\pi}{2} (r_p - t - r_w) \quad (5)$$

$$\frac{\partial W}{\partial l} = 0 \quad \text{and} \quad \frac{\partial^2 W}{\partial l^2} < 0 \quad (6)$$

Therefore, the elastic force has a local maximum value with respect to the belt length. In addition, the belt length that produces the local maximum value is not related to physical properties such as Young's modulus. These qualitative characteristics are consistent with the experiment results.

Solely from these results and theoretical discussion, the optimal crawler belt length cannot be ascertained for the funicular flexible crawler that runs in the large intestine. However, these experiment results suggest the importance of ascertaining the adequate crawler belt length to obtain high

elastic force and thereby realize a funicular flexible crawler that has high propulsion force.

#### IV. CRAWLER UNIT FOR TURNING

Next, the crawler unit for turning will be described. The crawler unit for turning is arranged at the flexible crawler head: it steers the crawler, enabling it to enter deeply into bending areas of the large intestine. This study evaluated the bending path performance of head crawlers with two belts and one belt. Results show how crawlers can pass through a bent portion of the rectum of the large intestine model (bending to the right).

First, we discuss the bending path performance of head crawlers theoretically. Fig. 10 portrays the schematic diagram that the crawler runs at the bending area of colon in the cases of one belt and two belts. In this situation, we assume that only the crawler belt contacts with the large intestine to simplify the discussion.

In the case of a single belt arranged only on the left side of the frame, as presented in Fig. 10(a), the head crawler thrust force  $f_{one\_x}$  in the  $x$  axis direction can be expressed as

$$f_{one\_x} = f_l \cos \theta_l \quad (7)$$

where  $f_l$  represents the magnitude of the frictional force vector acting on the right side of the crawler belt from the colon. Also,  $\theta_l$  denotes the angle between the  $x$  axis and the direction of the frictional force vector acting on the right side of the crawler belt from the colon. In this case, if  $\theta_l$  is greater than 0 deg and less than 90 deg, then the thrust force is obtainable in the right direction through frictional force  $f_l$ . Therefore, it can pass through the bent area curved to the right.

For two belts arranged on the left side and the right side, as presented in Fig. 10(b), the head crawler thrust force  $f_{two\_x}$  in the  $x$  axis direction can be expressed as the following equation.

$$f_{two\_x} = f_l \cos \theta_l + f_r \cos \theta_r \quad (8)$$

Therein,  $f_r$  represents the magnitude of the frictional force vector acting on the right side of the crawler belt from the colon. Also,  $\theta_r$  stands for the angle between the  $x$  axis and the direction of the frictional force vector acting on the right side of the crawler belt from the colon. When the left side belt and the right side belt are placed symmetrically with respect to the  $y$  axis,  $f_l = f_r$  and  $\theta_l = -\theta_r$ . Then  $f_{two\_x}$  becomes 0, rendering passage through the bent portion difficult.

Fig. 11 portrays the state of the respective paths in the cases of one belt and two belts. Experiment results show that the head crawler with two belts was unable to pass through the bent area. That with one belt passed through the bent section in about 15 s.

Based on the results presented above, only one belt of the top crawler was used. For bending to the left, if the shaft is rotated 180 deg by the operator's hand, then it can pass through the bent area on the same principle.

#### V. FUNICULAR FLEXIBLE CRAWLER

##### A. Prototype

Fig. 12 exhibits the flexible crawler prototype with a crawler

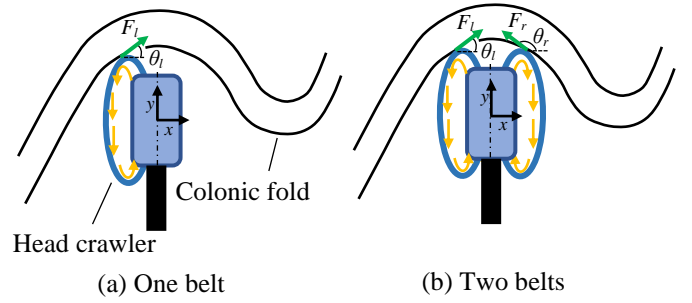


Fig. 10. Head crawler in a bending area of the large intestine.

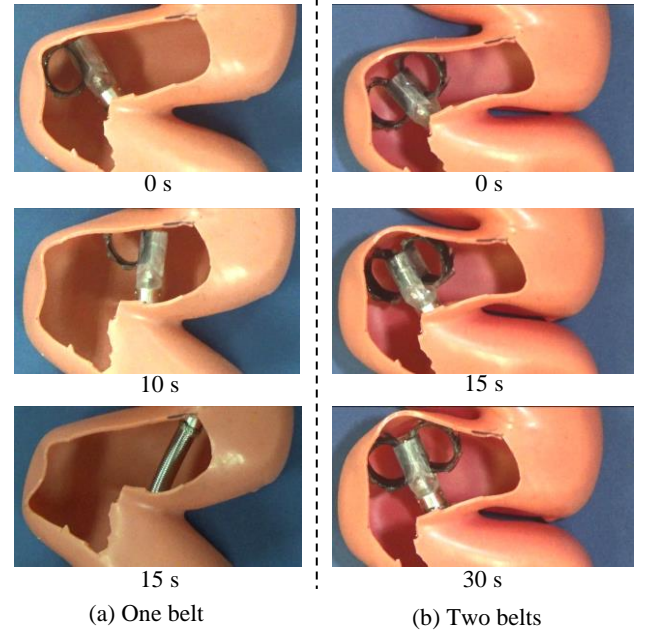


Fig. 11. Turn at the curved colon: (a) one belt and (b) two belts.

unit for propulsion and for turning. Table I presents its specifications. The prototype crawler has 1400 mm total length.

A crawler unit for propulsion and a crawler unit for turning have respective outer diameters of  $\phi 16.4$  mm and  $\phi 12.7$  mm when the crawler belt is deformed maximally. The flexible shaft outer diameter is  $\phi 8$  mm. This prototype consists mainly of three crawler units for propulsion, a crawler unit for turning, and an actuation unit. Because more than four crawler units for propulsion cause twist deformation of the flexible shaft because of the motor torque, three crawler units were selected for propulsion.

The crawler unit frame was molded of epoxy resin using stereolithography (Form2; Formlabs Inc.). In this crawler, the slip between the belt and the pipe/phantom was observed under all belt teeth conditions. The slip increases the insertion time and load on the colon. Therefore, the seven teeth belt that provides maximum friction was selected to reduce the slippage. The worm was an aluminum rod (A2017) produced using an NC milling machine. The flexible inner shaft (LB-2.1-2.5-2.9-2-0.2; Hagitec Inc.) and flexible outer shaft (LB-7.0-7.6-8.0-2.0-0.2; Hagitec Inc.) comprise a sleeve and a stainless steel thin sheet coil. The sleeve, formed by weaving narrow stainless steel wires, was arranged on the outer thin sheet coil. The actuation unit included a DC geared motor

(GP13ASL; Maxon Motor AG). The interval between the crawler unit for propulsion and the crawler unit for turning, and the interval between crawler units for propulsion were, respectively, 150 mm and 100 mm.

### B. Traction force

The crawler unit moves forward by the frictional force between the crawler belts and its ground contact surface. Therefore, the maximum traction force  $f$  of a crawler unit can be expressed as

$$f = \mu N \quad (9)$$

where  $\mu$  denotes the friction coefficient between the crawler belt and its ground contact surface.  $N$  denotes normal force acting on the ground surface from the crawler belt.

The flexible crawler generates greater traction force by connection of multiple crawler units to the flexible shaft as the total frictional force between the crawler belt and its ground contact surface increases. Traction force  $F_t$  of the flexible crawler with multiple crawler units is expressed as Eq. (10),

$$F_t = \sum_{i=1}^n f_i \quad (10)$$

where  $n$  represents the number of the crawler units connected to a flexible shaft.

We verified whether the traction force of the flexible crawler actually increases, or not, by increasing the number of crawler units. Fig. 13 presents an experimental system used to measure the flexible crawler traction force. The experiment, conducted with a  $\phi 28$  mm pipe fixed in the ground, measured the flexible crawler traction force using a force gage when driving in the pipe. The crawler belt of the crawler unit for turning was removed to measure the traction force of the crawler unit for propulsion. In addition, A lubricant was used in the pipe to simulate a wet condition.

Regarding measurements, the maximum traction force was measured five times for each condition. Then the average of five measurements was taken as the traction force measurement result. Fig. 14 presents the measurement result. The respective traction forces of one unit, two units, and three units were 0.67 N, 1.36 N, and 2.06 N. Results verified that the traction force of the flexible crawler increased almost linearly with increasing numbers of crawler units.

### C. Moving velocity

This flexible crawler was designed with multiple crawler units arranged on the flexible shaft to suppress the moving velocity loss caused by friction between the flexible shaft and its contact surface. Therefore, we verified whether the moving velocity loss is actually suppressed by increasing the number of crawler units, or not.

Fig. 15 presents an experimental system used to measure the flexible crawler speed. Three flexible crawlers were used in this experiment: one with a crawler unit for turning and a crawler unit for propulsion, one with a crawler unit for turning and two crawler units for propulsion, and one with a crawler unit for turning and three crawler units for propulsion. The experiment

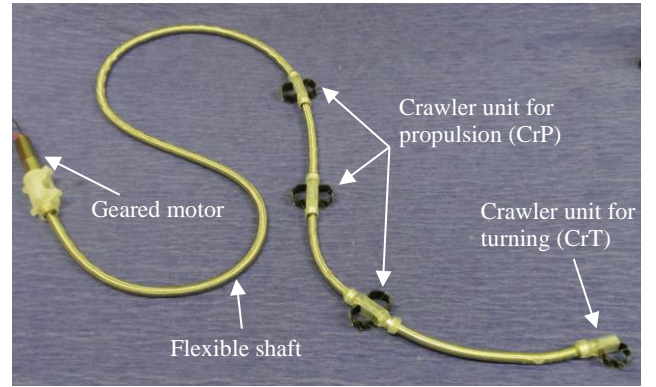


Fig. 12. Prototype of a funicular flexible crawler.

TABLE I. FUNICULAR FLEXIBLE CRAWLER PROTOTYPE SPECIFICATIONS

Total length	1400 mm
Weight	187 g
Motor	DCX14L 10.5W 103:1, Maxon Motor AG
Interval between crawler unit for propulsion and crawler unit for turning	150 mm
Interval between crawler units for propulsion	100 mm
Outer diameter of crawler unit for propulsion	$\phi 16.4$ mm
Outer diameter of crawler unit for turning	$\phi 12.7$ mm
Flexible shaft	
Outer diameter of outer flexible shaft	$\phi 8$ mm
Outer diameter of inner flexible shaft	$\phi 2$ mm
Crawler belt	
Material	silicone rubber
Width	9.0 mm
Height of belt part	1.5 mm
Height of tooth part	1.0 mm

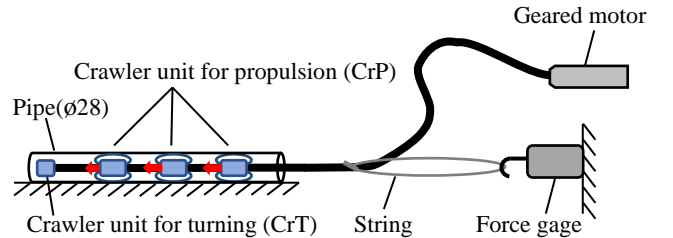


Fig. 13. System for measuring traction force of the funicular flexible crawler.

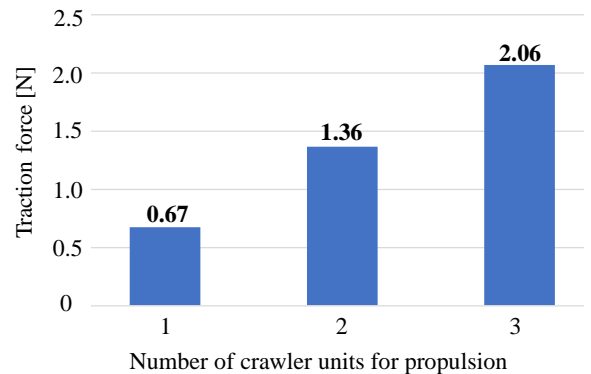


Fig. 14. Traction force of the funicular flexible crawler vs. crawler units used for propulsion.

was performed with the same prototype, but without engaging all crawlers. In the experiment, conducted with a T-shaped pipe of  $\phi 28$  mm fixed to the ground, time to reach the target of each flexible crawler was measured as it moved through the pipe. Measurement was started when the head crawler unit reached the end of a straight pipe positioned in front of a tee. It was terminated when the head crawler unit reached 500 mm from the tee. A lubricant was used in the pipe to simulate a wet condition. The rotating speed of the gear motor was set as 2000 r/min for all flexible crawlers. Time to reach the target was measured five times for each condition. Then the average of five measurements was taken as the time to reach the target measurement result.

Fig. 16 presents the measurement results. Results verify that the time to reach the target decreased concomitantly with an increasing number of crawler units used for propulsion. Multiple crawler units reduced the slip between the crawler belts and the pipe. The results presented above demonstrate that increasing the number of crawler units is effective for improving propulsion performance.

#### D. Phantom Insertion Experiment

Examining the entire large intestine requires insertion of the colonoscope tip up to the cecum. In addition, the actual large intestine is extremely soft and movable, with a complicated shape. For that reason, medical students and young doctors often use the silicone rubber large intestine phantom for insertion training. Its shape and compliance resemble those of actual large intestines. For this study, we conducted insertion experiments using a large intestine phantom (M40 11361-000, Kyoto Kagaku Inc.) to verify the usefulness of this flexible crawler. Results of this experiment verified the relation between the crawler unit number and the insertable distance.

The silicone rubber large intestine phantom consists of an anus part, rectum part, the sigmoid colon part, the descending colon part, the transverse colon part, the ascending colon part, and the cecum part. Regarding the phantom specification used for this study, the phantom total length from the anus to the cecum is about 1000 mm. The phantom inner diameter between the rectum and the cecum is 28–55 mm. The anus part inner diameter is 20 mm. The phantom thickness is about 1.4 mm. A lubricant was used in the pipe to simulate a wet condition.

The flexible crawler was inserted from the anus to the cecum. In the phantom insertion experiment, the operator knows which direction to rotate the device by the LED light installed in the crawler head. Four flexible crawlers were used with the moving velocity experiment described above. The experiment was conducted three times for each condition. The flexible crawler runs inside the phantom using the traction force generated by the crawler unit for propulsion. At the bent area, it steers using the steering mechanism by the crawler unit for turning as described in section IV. The gear motor rotation rate was set as 2000 r/min for all flexible crawlers.

Fig. 17 and Table II present experiment results obtained for phantom insertion. Results suggest that increasing the number of crawler units is effective for improving the propulsion performance inside the large intestine phantom. In addition,

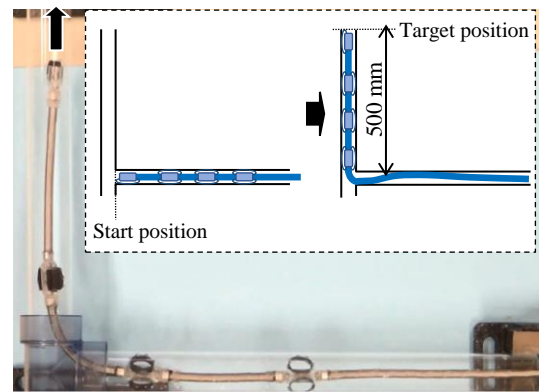


Fig. 15 Running the funicular flexible crawler in an L-shaped pipe.

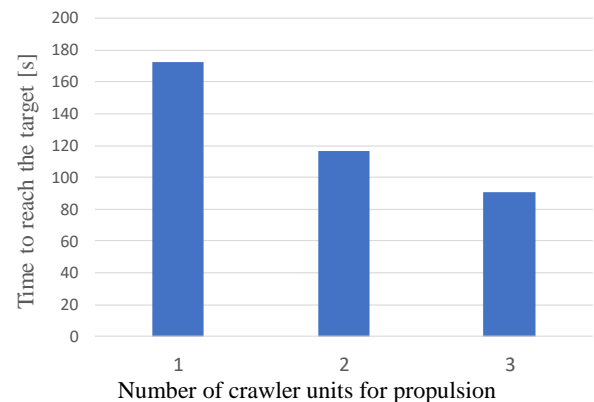


Fig. 16. Time to reach the target vs. the number of crawler units.

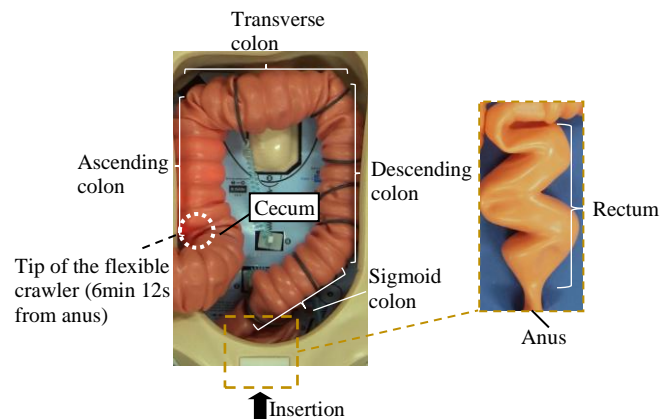


Fig. 17. Phantom insertion experiment of a prototyped funicular flexible crawler.

TABLE II  
EXPERIMENT RESULT OF PHANTOM INSERTION: CrT AND CrP DEPICT CRAWLER UNIT FOR TURNING AND CRAWLER UNIT FOR PROPULSION.

Number of units		Rectum	Sigmoid colon	Descending colon	Transverse colon	Ascending colon	Cecum
CrT	CrP						
1	0						
1	1						
1	2						
1	3						

results demonstrated reported that the flexible crawler head reached the cecum when three crawler units were used for propulsion. The flexible crawler head reached the cecum in about 6 min. That performance seems to be sufficient because conventional colonoscopy lasts approximately 45 min for an entire procedure [22]. Future works will conduct an ex vivo insertion test to demonstrate the effectiveness of the flexible crawler for colonoscopy.

## VI. CONCLUSION

As described herein, we proposed the funicular flexible crawler mechanism and described its expected applicability to colonoscopy as a first step for this study. Our conclusions and future works can be summarized as follows:

- (1) The proposed crawler comprises a flexible shaft attached to a multiple crawler unit and a geared motor. Miniaturization of the outer diameter ( $\phi 16.4$  mm) of the device was achieved.
- (2) Experiment and theoretical analysis confirmed a qualitative relation between the crawler belt length and the elastic force. Based on this result, it is expected that a model with consideration of the deformability of colon tissues and the relative movement of the lumen is constructed for optimization of the belt.
- (3) In-pipe running experiments show that the number of crawler units increases the traction force and the moving velocity. The relation between the belt slip velocity and the traction force, or between the belt slip velocity and the friction force of the scope in the pipe, must be examined more deeply in future studies.
- (4) Phantom insertion experiments demonstrated that increasing the number of crawler units is effective for improving propulsion performance. The flexible crawler with a crawler unit for turning and three crawler units for propulsion was able to run from the rectum to the cecum.

In the future, practical design for diagnosis, and clinical evaluation are also expected. Regarding practical design, the flexible crawler has no device for diagnosis or for MIS yet. Nevertheless, because the flexible crawler is a wired scope and not a capsule, adding such a device would presumably be easier to accomplish than if one were to use a capsule. It is important to realize that the single bend on the tip can manage left and right angles after applying roll of the entire scope. That can realize colon inspection and can reduce pain for the patient and enable diagnosis behind the bends. Such a steering system must be constructed for future study. Regarding clinical evaluation, the crawler belt edge might damage colon tissue by the scope or belt rotation. It is important to demonstrate that the flexible crawler does not damage actual colon tissue.

## REFERENCES

- [1] GLOBOCAN 2018, International Agency for Research on Cancer 2019. Available from: <https://gco.iarc.fr/>, accessed on 19/01/2019.
- [2] S. Lee, Y. Park, D. Lee, and K. Kim, "Colonoscopy procedural skills and training for new beginners." *World Journal of Gastroenterol.*, Vol. 20, No. 45, pp. 16984-16995, 2014.
- [3] Y. Jung and S. Lee, "How Do I Overcome Difficulties in Insertion?" *Clinical Endoscopy*, Vol. 45, No. 3, pp. 278–281, 2012.
- [4] P. Valdastrì, et al. "Magnetic air capsule robotic system: proof of concept of a novel approach for painless colonoscopy." *Surgical Endoscopy*, Vol. 26, No. 5, pp. 1238-1246, 2012.
- [5] G. Pan and L. Wang, "Swallowable Wireless Capsule Endoscopy: Progress and Technical Challenges," *Gastroenterology Research and Practice*, 2012, pp. 1-9.
- [6] Sliker, Levin J., and Gastone Ciuti, "Flexible and capsule endoscopy for screening, diagnosis and treatment." *Expert Review of Medical Devices* Vol. 11, No. 6, pp. 649-666, 2014.
- [7] D. Glozman, N. Hassidov, M. Senesh, and M. Shoham, "A Self-Propelled Inflatable Earthworm-Like Endoscope Actuated by Single Supply Line," *IEEE Transactions on Biomedical Engineering*, vol. 57, 2010, pp. 1264-1272.
- [8] K.D. Wang, G.Z. Yan, P.P. Jiang, and D.D. Ye, "A wireless robotic endoscope for gastrointestinal," *IEEE Transactions on Robotics*, vol. 24, no. 1, pp. 206-210, Feb. 2008.
- [9] Y.P. Lee, B. Kim, M.G. Lee, and J. Park, "Locomotive mechanism design and fabrication of biomimetic micro robot using shape memory alloy," in: *Proc. IEEE International Conference on Robotics and Automation*, pp. 5007-5012, Apr. 2004.
- [10] J.E. Bernth, A. Arezzo, and H. Liu, "A Novel Robotic Meshworm With Segment-Bending Anchoring for Colonoscopy." *IEEE Robotics and Automation Letters*, Vol. 2, No. 3, pp. 1718-1724, 2017.
- [11] F. Cosentino, E. Tumino, GR. Passoni, E. Morandi, A. Capria, "Functional evaluation of the endotics system, a new disposable self-propelled robotic colonoscope: in vitro tests and clinical trial," *Int J Artif Organs*, Vol. 32, pp.517-527, 2009.
- [12] J.O. Alcaide, L. Pearson, and M.E. Rentschler, "Design, modeling and control of a SMA-actuated biomimetic robot with novel functional skin." 2017 IEEE International Conference on Robotics and Automation, pp. 4338-4345, 2017.
- [13] T. Nakamura, Y. Hidaka, M. Yokojima, and K. Adachi, "Development of Peristaltic Crawling Robot with Artificial Rubber Muscles Attached to Large Intestine Endoscope," *Advanced Robotics*, vol. 26, pp. 1161-1182, 2012.
- [14] S. Wakimoto and K. Suzumori, "Fabrication and basic experiments of pneumatic multi-chamber rubber tube actuator for assisting colonoscopy insertion," in: *Proc. IEEE Int. Conf. on Robotics and Automation (ICRA 2010)*, 2010, pp. 3260-3265.
- [15] J. Nagase, Japanese Patent, JP 6109643, 2013.5.21.
- [16] J. Nagase, K. Suzumori, and N. Saga, "Development of Worm-Rack Driven Cylindrical Crawler Unit," *Journal of Advanced Mechanical Design, Systems, and Manufacturing*, vol. 7, no. 3, pp. 422-431, 2013.
- [17] A. Singh, E. Sachdeva, A. Sarkar, and K. M. Krishna, "COCrIP: Compliant OmniCrawler in-pipeline robot," *IEEE/RSJ International Conference on Intelligent Robots and Systems (IROS)*, pp. 5587-5593, 2017.
- [18] J. Kim, G. Sharma, and S. Iyengar, "FAMPER: A Fully Autonomous Mobile Robot for Pipeline Exploration," in: *Proc. 2010 IEEE /ICIT International Conference on Industrial Technology*, Vina del Mar, 2010, pp. 517-523.
- [19] J. Borenstein, M. Hansen, and A. Borrell, "The OmniTread OT-4 Serpentine Robot 1 – Design and Performance," *Journal of Field Robotics*, vol. 24, no. 7, pp. 601-621, 2007.
- [20] F. Fukunaga and J. Nagase, "Cylindrical elastic crawler mechanism for pipe inspection inspired by amoeba locomotion," in: *Proc. 2016 Sixth IEEE International Conference on Biomedical Robotics and Biomechanics (BioRob)*, pp. 424-429, 2016.
- [21] R.J. Roark and W.C. Young, "Formulas for Stress and Strain," Fifth ed., New York: McGraw-Hill, 1975.
- [22] P. B. Cotton et al., "Colonoscopy: Practice variation among 69 hospital-based endoscopists," *Gastrointestinal Endoscopy*, vol. 57, no. 3, pp. 352–357, 2003.